FOURTH AUSTRALASIAN CONFERENCE
on
HYDRAULICS AND FLUID MECHANICS
at
Monash University, Melbourne, Australia
1971 November 29 to December 3

WAKE FLOWS BEHIND TWO-DIMENSIONAL SQUARE CYLINDERS AT LOW REYNOLDS NUMBERS

by
K. P. STARK*

S U M M A R Y

Solutions of the Navier-Stokes equations - steady, laminar and two-dimensional including inertia terms - have been obtained using the Vorticity Transport equations for flow patterns around infinite arrays of square cylinders at right angles to the flow direction.

The proportions of the problem have been varied to give rectangular cavity sizes over a wide range such that results have been obtained for porosities ranging from .36 to .97 and for cavity ratios (distance between cylinders/ half length of square cylinder side) from 0.5 to 10.0.

Solutions have been obtained for low Reynolds number with inertia terms retained and the position of the separating streamline is defined automatically by the solution. The development of the vortex patterns in the wake region with increasing flow (RN) and with varying cavity proportions clearly illustrates some interesting circulation patterns in the separated flow region.

The results for the creeping flow regime are compared with those of other workers.

*K.P. Stark, Associate Professor in Engineering, James Cook University of North Queensland, Townsville, Australia.

INTRODUCTION

The study of flow patterns behind a series of bluff bodies has important applications in bioengineering, aeronautics, meteorology, textile technology and chemical, civil and nuclear engineering. Using idealised models, calculations can be performed on present day computers at a rate which allows the effect of the various parameters to be involved. Combinations of such solutions should eventually yield an all embracing solution for the complex nonhomogeneous wake flows found in practice.

The study described in this paper is concerned with flow past infinite arrays of square cylinders arranged in a rectangular lattice as illustrated in Figure 1. This model has been adopted as an idealisation of a porous medium in which variations in porosity (and therefore cavity dimensions) may be introduced. The fluid considered is assumed to be Newtonian and incompressible whereas the flows are treated as steady and isothermal at low Reynolds numbers (RN). The solutions incorporate laminar flow inertia terms and range from creeping flows (RN = 0) to flows where the inertia terms are of considerable importance.

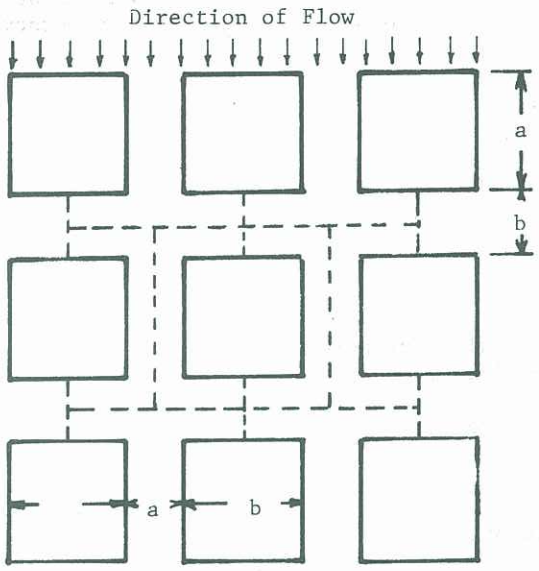

FIGURE 1. The 2-D Porous Medium Model.

Thom and Apelt (1) analysed the pressure distribution in a two-dimensional static hole at low Reynolds numbers in 1957. Since then a number of studies of cavity flows have appeared in the literature. These have included the analytical and numerical work by O'Brien (2,7), Mehta and Lavan (3) and Hung and Macagno (4) and the experimental studies by Weiss and Florsheim (5) and Pan and Acrivos (6). O'Brien (7) summarises most of these studies.

If the idealised porous medium of Figure 1 is assumed infinite in extent, a typical bay to be analysed is shown as Figure 2a. For comparison a typical flow domain used in O'Brien's studies (7) of creeping flows over rectangular cavities with either Couette or Poiseuille characteristics is shown as Figure 2b. The principal differences between the two models are

(a) inertia terms are retained in Figure 2a but not in the creeping flow studies of Figure 2b, thus, an additional boundary of symmetry which effectively halves the flow field exists in Figure 2b. For zero Reynolds

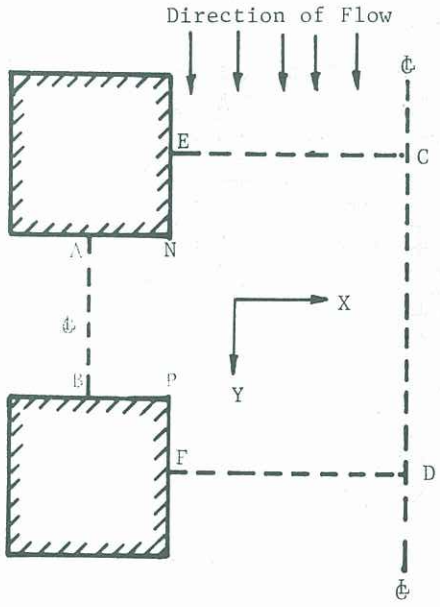

Figure 2a. A typical bay of the porous medium model (Stark 1968).

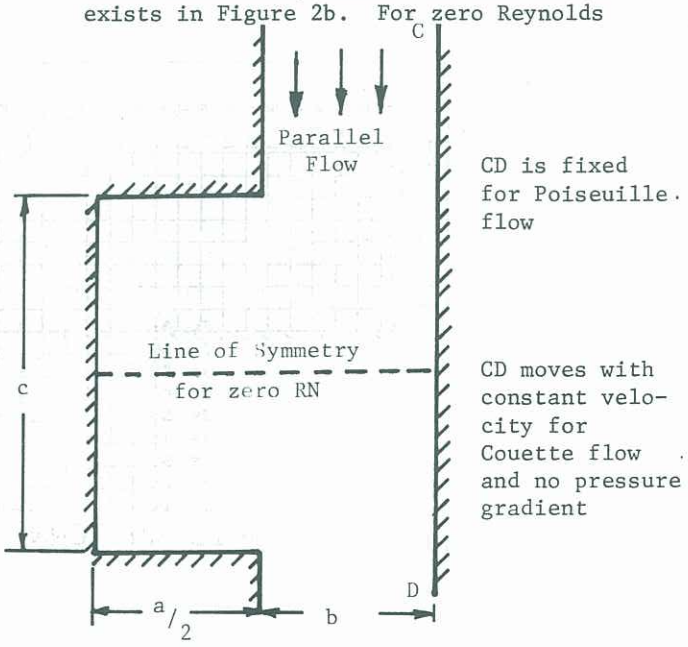

Figure 2b. Poiseuille and Couette flow model (O'Brien 1970).

number the typical bay of Figure 2a would also be halved by a horizontal line of symmetry.

(b) The cavity base is a rigid boundary for the Couette and Poiseuille flows of Figure 2b but a line of symmetry, AB , in Figure 2a.

(c) Figure 2b is bounded by a rigid boundary (stationary for Poiseuille, moving for Couette flow) whereas the corresponding boundary, CD , in Figure 2a is a line of symmetry between rows of fixed (square) cylinders.

SOLUTION OF THE FLOW EQUATIONS

The flow patterns within the appropriate boundaries can be resolved by a numerical technique applied to the fundamental equations for the flow - the Navier-Stokes equations. One of the most popular methods for such solutions involving two-dimensional, steady flows is the squaring technique outlined by Thom and Apelt (8). The application of this method to the problem considered is described by Stark (9,10) and involves the successive solution of the coupled second order vorticity-transport equations (equations 1 and 2) for the streamfunction (ψ) and the vorticity (ε) at each mesh point in the flow field until the field values so obtained satisfy the finite difference equations at each node point to a desired accuracy.

$$\nabla^2\psi = \varepsilon \qquad \ldots(1)$$

$$\nabla^2\varepsilon = RN\left(\frac{\partial\psi}{\partial x}\cdot\frac{\partial\varepsilon}{\partial y} - \frac{\partial\psi}{\partial y}\cdot\frac{\partial\varepsilon}{\partial x}\right) \qquad \ldots(2)$$

where ψ is a dimensionless streamfunction defined by $u = -\frac{\partial\psi}{\partial y}$, $v = \frac{\partial\psi}{\partial x}$.

ε is a dimensionless vorticity.

$RN = \frac{UL}{\nu}$

U is a representative velocity of the flow, which for porous media flows is generally taken as the seepage velocity.

L is a representative dimension; 'a' in Figure 1.

ν is the fluid kinematic viscosity.

u is the velocity component in the x-direction.

v is the velocity component in the y-direction.

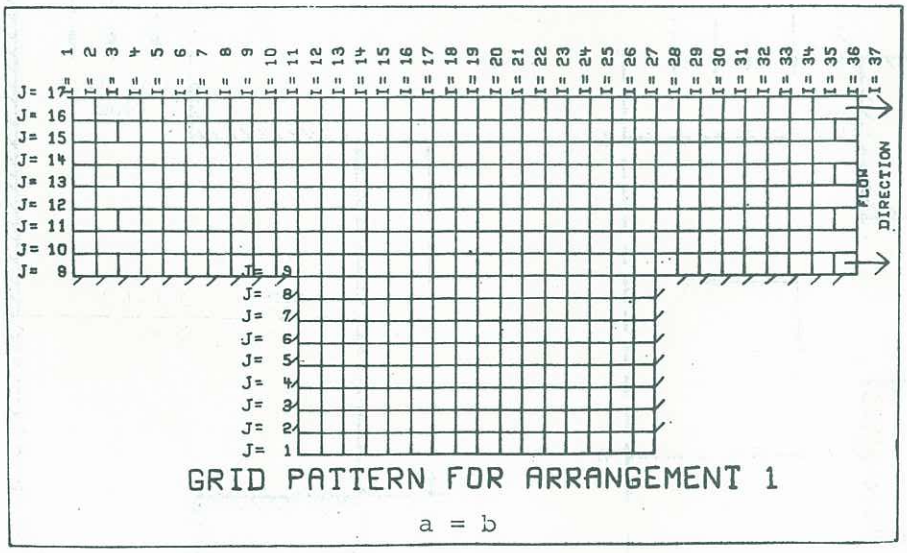

FIGURE 3. A typical grid pattern for the porous medium model.

A typical grid pattern showing the mesh size is illustrated in Figure 3. Decreasing the mesh size generally gives improved numerical accuracy; however, there is a need to optimise the computational requirements (memory size and available computer time) with respect to the desired accuracy.

The boundary conditions may be defined with reference to Figure 2a as:-

(a) AB and CD are streamlines (i.e. have a constant value of ψ) and lines of symmetry in the direction of flow (i.e. $\varepsilon = 0$).
(b) ENA and BPF are rigid boundaries with no slip (i.e. ψ = constant and ε must be calculated using no slip conditions).
(c) EC and FD have similar flow patterns about them and therefore changes in ψ and ε for flow approaching or leaving one of these lines must be identical with the corresponding changes about the other line, i.e. reciprocal symmetry.

RANGE OF SOLUTIONS

The idealised porous medium model was examined for a variety of porosities to determine the variation in head loss with porosity at different Reynolds numbers. The ranges considered for (i) RN (defined in terms of seepage velocity and the side, a , of the square cylinder), (ii) ratio of a/b in Figure 1 and (iii) porosity, are shown in Table 1. Beyond these ranges of RN numerical stability problems appeared and the solutions became unweildy.

TABLE 1

Porosity	Ratio a/b	Range of RN
.360	4.0000	0- 80.00
.555	2.0000	0-133.00
.750	1.0000	0-500.00
.840	0.6667	0- 80.00
.889	0.5000	0- 66.67
.918	0.4000	0- 57.14
.937	0.3330	0- 50.00
.960	0.2500	0- 40.00
.972	0.2000	0- 33.33

At the higher Reynolds numbers the flow pattern began to approach very closely that of parallel flow confined to a channel of width 'b' (Figure 1). This is associated with the movement of the separation streamline towards the body of the flow. Under these circumstances it seems pertinent to consider parallel Poiseuille flow for comparison purposes. Indeed, considerations of accuracy, convergence criteria, etc. were based on a detailed examination of the behaviour of the computer programs and the resultant solutions for the simple Poiseuille case of parallel flow. Obviously, the piezometric head drop across a typical bay of the porous medium model will be less than that in a channel of width 'b' and the difference will be a function of porosity. If the piezometric head drop across one bay of Figure 2a is defined as 'i' and the corresponding head loss for Poiseuille flow across a parallel channel of width 'b' and the same length as the porous medium bay is defined as i_p then a relative head loss coefficient for the porous medium bay is given by

$$\text{Relative head loss coefficient} = \frac{i}{i_p} \qquad \ldots(3)$$

Figure 4 shows the variation of this coefficient with porosity for zero Reynolds numbers. The plotted points agree very well with those obtained by O'Brien (7).

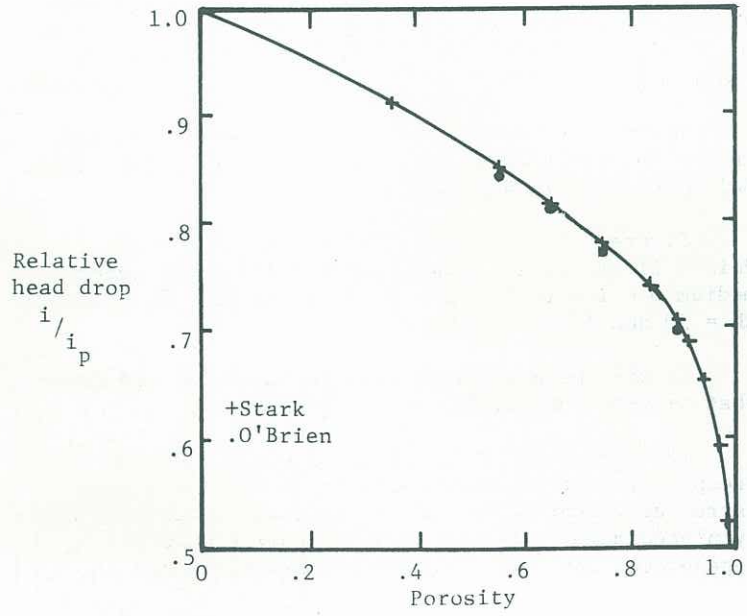

FIGURE 4. Relative head-loss coefficient v. porosity at RN = 0.

Head-loss coefficient = i/i_p.
Porosity = Volume of voids/total volume.

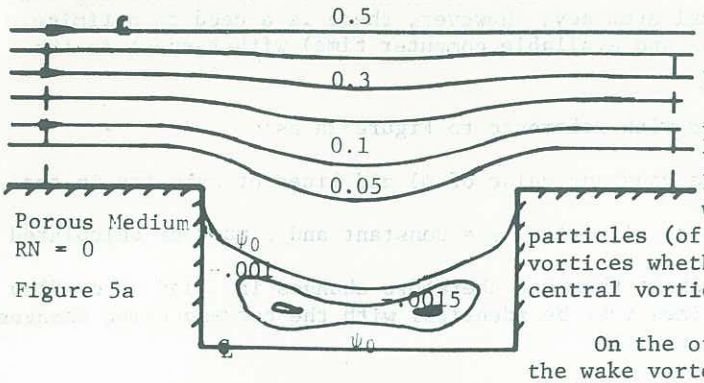

Figure 5a

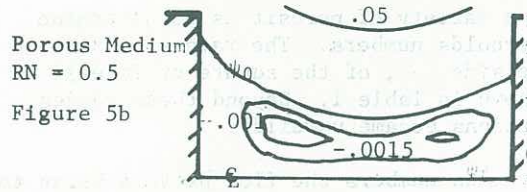

Figure 5b

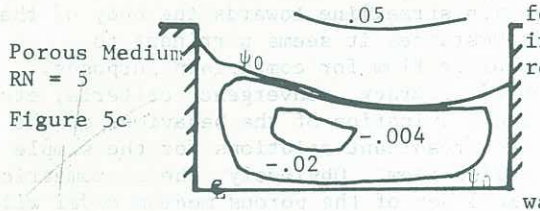

Figure 5c

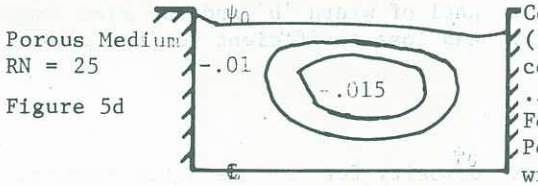

Figure 5d

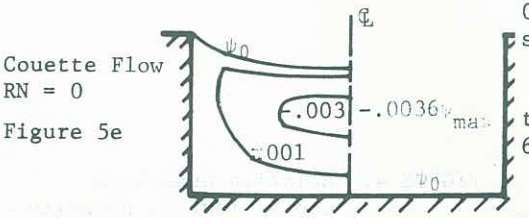

Figure 5e

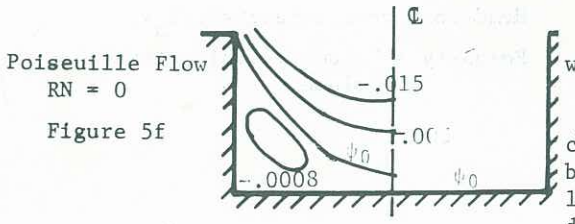

Figure 5f

FIGURE 5. Solutions for a = b models, porosity = 0.75.

FLOW IN THE WAKE REGION

In studying the wake region the position of the separation streamline ($\psi = 0$), the strength of the vortex pattern developed and the position of the vortex core are all important parameters. For zero Reynolds number comparatively weak vortex patterns exist between the particles (of porous medium) and the patterns of these vortices whether (multiple) central vortices or non-central vortices are always symmetrically aligned.

On the other hand, for non-zero Reynolds numbers the wake vortex patterns and the flow patterns generally become asymmetrical under the action of inertia terms. At the upper limits of Reynolds numbers considered the wake bubble remains asymmetrical whilst the main body of the flow approaches parallel flow. Thus, at these high Reynolds numbers the vortex pattern virtually fills the cavity between the blocks with the dividing streamline parallel to the base of the cavity. Only under these conditions does it appear reasonable to simulate the flow as a cavity box flow with the lid of the box moving. In the creeping flow range, the dividing streamline is seen to dip into the cavity and for large porosities (i.e. small a/b ratios) the dividing streamline may even intersect the line of symmetry representing the base of the cavity.

SOME CREEPING FLOW WAKE PATTERNS

It is interesting to compare the formation of the wake region flow for the three different boundary conditions which will be referred to as (i) porous medium model, (ii) Couette flow model and Poiseuille flow model (see Figures 2a and 2b). The solutions for the Couette and Poiseuille models are taken from O'Brien (7) and the three ratios of a/b viz a/b = 4,2,1 are compared. These cases correspond to porosities of .36, .56 and .75 respectively for the porous medium model. For the two models to be comparable the Couette and Poiseuille flow models are considered for the geometry with c = b in Figure 2b.

Solutions for a/b = 1 are given as Figure 5 with (5a) to (5d) being the porous medium model for RN = 0, 0.5,5 and 25, and Figures 5e and 5f being O'Brien's solutions for Couette and Poiseuille flows respectively.

Figure 6 shows the porous medium model (Fig.6a), the Poiseuille flow (Fig.6b) and the Couette flow (Fig. 6c) model for a/b = 2 and for zero RN.

Figure 7 illustrates solutions for a/b = 4, Poiseuille (Fig.7a), Couette (Fig.7b) and the porous medium model (Fig.7c) RN = 0, (Fig.7d) RN = 8, (Fig.7e) RN = 50 and (Fig.7f) RN = 80.

It will be noted that the flow profiles are somewhat similar for similar cavity geometries.

If a/b = 1 (Figs.5a,5e,5f) is considered for creeping flow the porous media model gives a double barrelled vortex whilst the Couette model has a centrally placed main vortex and the Poiseuille model has degenerated into two discrete corner vortices.

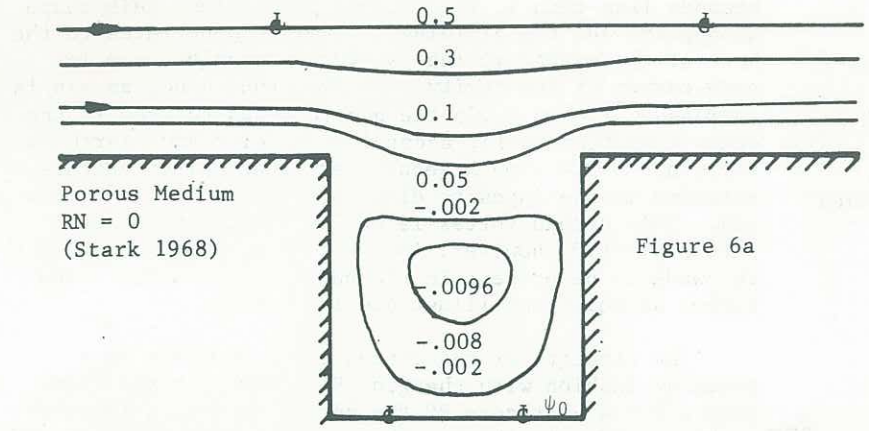

Figure 6a

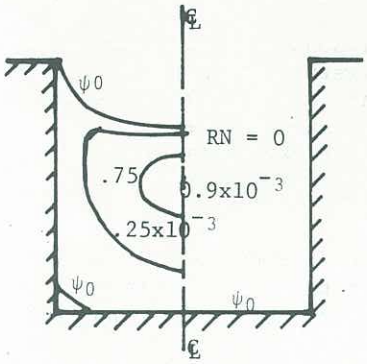

Figure 6b

O'Brien
(1970)

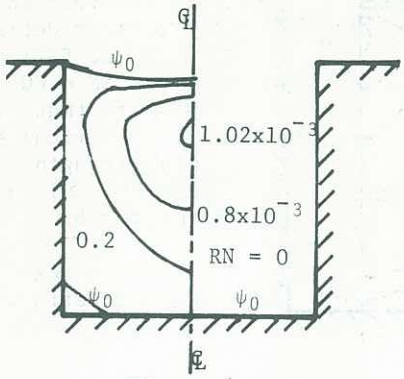

Figure 6c

FIGURE 6. Porous Medium Model (6a), Poiseuille (6b), Couette (6c) for a/b = 2, Porosity = 0.56.

For a/b = 2, Figures 6, a central vortex exists for each set of boundary conditions and very weak corner vortices are also present.

When a/b = 4 the creeping flow solutions (Figures 7a,7b,7c) each show two central vortex patterns although at zero RN the size of the vortex cannot be determined if streamfunctions are evaluated to four significant figures.

Table 2 summarises the vortex core streamfunction values and it is seen that for a/b = 2 and 4 the value is approximately the same for each model whereas for a/b = 1 the porous media model value is again intermediate between the Poiseuille and Couette flows.

It should be noted that the dividing streamline for similar cavity geometry penetrates more deeply into the cavity for Poiseuille and porous media flows than for the Couette profile and in all cases the assumption of a parallel dividing streamline would be quite erroneous.

TABLE 2

VORTEX CORE VALUES FOR CREEPING FLOW

Values given are $\psi_{max} \times 10^2$.

a/b	Porous Media	Poiseuille	Couette
4	0.987	1.00	1.05
2	0.963	0.90	1.02
1	0.150	0.08	0.36

WAKE PATTERN VARIATIONS WITH REYNOLDS NUMBER

The numerical solutions for the porous media model for a/b = 1 and a/b = 4 are given in Figures 5 and 7 and the variation with Reynolds number for these geometries can be readily seen by comparing solutions for increasing RN. Reynolds number has been based on the particle size 'a' (Figure 2a) and the seepage velocity which is given by the (total flow/full cross section area).

The following features of the wake flow are evident in the plotted contours -

At zero Reynolds number the flow pattern is symmetrical about a line normal to the direction of flow and situated midway between the particles. This symmetry is achieved because the inertia terms vanish for creeping flows. For the patterns with a porosity greater than 0.80 the numerical results do not indicate the presence of a wake vortex at zero RN but it appears certain that a finer grid and a greater number of significant figures would show the presence of very weak corner vortex patterns.

As Reynolds number increases the flow pattern becomes asymmetrical. In all cases the centre of the vortex moves upstream initially but, at still higher flow the centreline tends to move downstream, crossing the axis of symmetry (for zero RN), and moving into the downstream half of the wake area. This movement of the vortex is dependent on the shape of the dividing streamline. Although the streamfunction contour is symmetrically placed at zero RN it becomes asymmetrical as RN increases, being nearer the base of the cavity in the downstream half of the cavity. At this stage the main channel flow is not moving fast enough to bypass the cavity, however, at even higher RN's the comparatively fast flowing main channel flow approaches parallel flow and the vortex in the cavity moves downstream as if carried by the mainstream. As the centre of the wake vortex moves downstream it also moves further away from the base of the cavity. For a = b, at zero RN, the bubble appears to have a doublebarrelled shape and as a/b

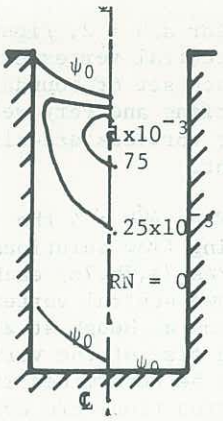

Figure 7a

Poiseuille
O'Brien (1970)

becomes less than 1, i.e. higher porosities, this shape disappears and the dividing streamline penetrates to the base of the cavity giving two vortex bubbles, one in each corner of the cavity. On the other hand, as a/b is increased, i.e. n < .75 the bubble tends to grow in the other direction until, according to Weiss and Florsheim (5), a/b = 3.4 when a second very weak vortex appears, rotating in the opposite direction to the dominant vortex. This second vortex is obvious in the solutions with a/b = 4.0, however, in the zero RN solution it is too weak to be present in the numerical solution. The higher RN solutions illustrate it clearly.

The strength of the vortex cores develops in a peculiar fashion with changing RN. Consider the flows with a/b = 4 - at zero RN the second vortex is too weak to be recorded in the fourth decimal place. However, at RN = 8 it is definitely present although very weak. At RN = 40 and 50 it appears to reach its peak value because at RN = 80 the vortex reverts to a pattern quite similar to that for zero RN with only one vortex evident in the numerical solution. This vortex does have a higher strength for the RN = 80 flow. Weiss and Florsheim (5) indicate that a third vortex develops when a/b = 8.

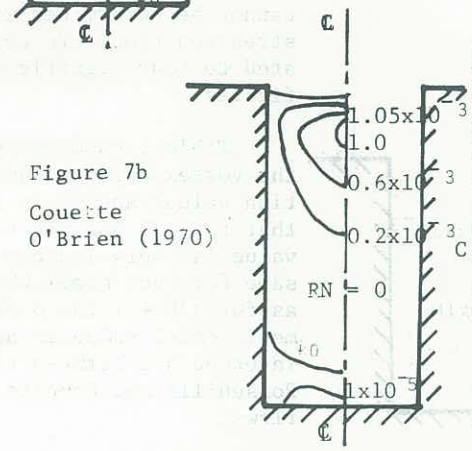

Figure 7b

Couette
O'Brien (1970)

The vortex core strength of a number of the vortices are defined in Table 3 in terms of the stream-function value of the core. These properties cannot be compared directly with the analytical results of Weiss and Florsheim (5) because of their assumption that the dividing streamline is parallel to the base of the cavity from corner to corner of the blocks. As their analyses were restricted to zero RN flows this assumption is obviously incorrect as evidenced by the zero RN contour plots.

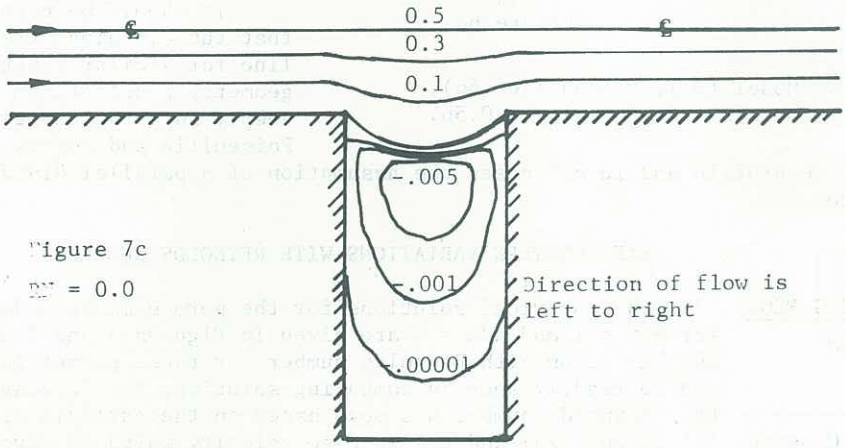

Figure 7c

RN = 0.0

Porous Medium Models a/b = 4

Figure 7d

RN = 8

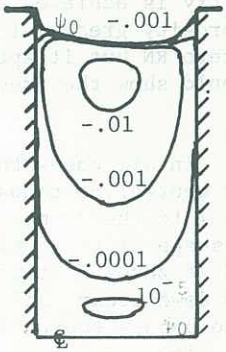

Figure 7e

RN = 50

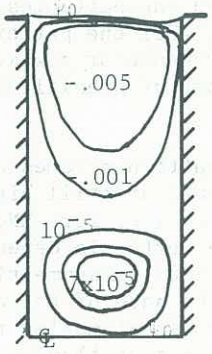

Figure 7f

RN = 80

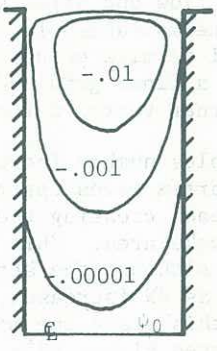

FIGURE 7. Solutions for a/b = 4, porosity = 0.36, Poiseuille (7a), Couette (7b), Porous Medium (7c,d,e,f).

TABLE 3

PROPERTIES OF CAVITY VORTICES

a/b	Porosity	RN	Vortex Core Value
4.00	.36	0	.00001,-.00990
		40	.00002,-.02500
		80	-.03200
2.00	.56	0	-.00960
		33.33	-.02600
		133.30	-.02900
1.00	.75	0 (2 at)	-.00157
		25	-.01900
		100	-.02300
0.50	.89	16.66	-.00009,-.00400
		66.66	-.01160
0.25	.96	10	-.00027
		40	-.00190

The experiments of Weiss and Florsheim, on the other hand, do support the higher RN solutions obtained for the porous media model. These experiments placed the vortex core at a height of .65 depth above the cavity base for RN_{WF} = 150 and a/b = 2 where

$$RN_{WF} = \frac{V_W \times D_W}{\nu}$$

and V_W = free streamline velocity assumed above cavity.

D_W = distance from stagnation point to separation point.

The porous media solutions for the same geometry at RN = 33, 50, 66 and 133 give a height to centre of vortex of 0.71 of the cavity depth.

CONCLUSION

Cavity flows are particularly important when considering the fundamental characteristics of flow in porous materials. The nature of heat and mass transfer made possible by cavity type vortex patterns behind particles (cells) in the micro-circulation have important biological implications. Fluidization problems, sediment transportation, scouring of a river bed and measurement of the texture of fleeces and fabrics - all require an understanding of cavity flow behaviour before a detailed analysis of the natural problem can be undertaken.

The numerical solutions presented here represent an approach to the problem which has become practicable with the advent of present day computational facilities. Non-linear flow characteristics can be included without special problems. Additional experimental work is required to show conclusively the accuracy of the results. All evidence available appears to show agreement with the numerical results. The numerical solutions provide details of all the flow characteristics including velocity and pressure distributions, and vortex patterns. Such details cannot easily be measured experimentally particularly at low Reynolds numbers.

More complex boundary geometries and even three-dimensional problems can be attacked in a similar fashion but inevitably will require more detailed programming, computer time and capacity. Higher Reynolds numbers may be included and non-rigid boundaries can be treated in unsteady problems using a marker and cell technique (12) however such problems require computational facilities - of time and memory size - at least one order of magnitude above the requirements of the problems discussed in this paper.

BIBLIOGRAPHY

(1) THOM, A. and APELT, C.J.A. (1958) Aeron. Res. Council R & M No.3090, H.M.S.O.

(2) O'BRIEN, V. (1966) Technical Memo TG-814 Johns Hopkins University, March 1966.

(3) MEHTA, U.B. and LAVAN, Z. (1969) NASA Rept. CR-1245.

(4) HUNG, T.K. and MACAGNO, E.O. (1966) La Houille Blanche, p.397.

(5) WEISS, R.F. and FLORSHEIM, B.H. (1965) Jnl. Physics Fluids 8(9):1631-1635.

(6) PAN, F. and ACRIVOS, A. (1967) Jnl. Fl. Mech., 28, p.643.

(7) O'BRIEN, V. (1970) Technical Memo TG-1138 Johns Hopkins University, October 1970.

(8) THOM, A. and APELT, C.J.A. (1961) Field computations in engineering and physics, D. Van Nostrand Co. Ltd.

(9) STARK, K.P. (1969) IAHR Symposium, Hafia, February 1969.

(10) STARK, K.P. (1969) Proc. IASH/AIHS-UNESCO Conf., Tucson, Pub.No.80, Vol.2, p.635-649.

(11) HARLOW, F.H. (1964) The particle-in-cell computing method for fluid dynamics. Methods in Computational Physics, Acad. Press, 3:319-343.